Numerical Model of Dog Mast Cell Tumor Treated by Electrochemotherapy

*Daniela O. H. Suzuki, *Jânio Anselmo,†Krishna D. de Oliveira, †Jennifer O. Freytag,†Marcelo M. M. Rangel, *Jefferson L. B. Marques, *§Airton Ramos.

*Institute of Biomedical Engineering, Federal University of Santa Catarina (UFSC); †Oncology Veterinary, Vet Cancer; §Department of Electrical Engineering, State University of Santa Catarina (UDESC).

Abstract: Electrochemotherapy is a combination of high electric field and anticancer drugs. The treatment basis is electroporation or electropermeabilization of cell membrane. Electroporation is a threshold phenomenon and, for efficient treatment, an adequate local distribution of electric field within the treated tissue is important. When this local electric field is not enough, there is a regrown tumor cell; however, if it is stronger than necessary, permanent damage to the tissue occurs. In the treatment of dogs, electrochemotherapy is not yet an established treatment for mast cell tumor in veterinary medicine, although there are studies showing evidence of its effectiveness. In this study, we examined electrochemotherapy of dog mast cell tumor with numerical simulation of local electric field distribution. The experimental result was used to validate the numerical models. The effect of tumor position and tissue thickness (tumor in different parts of dog body) was investigated using plate electrodes. Our results demonstrated that the electrochemotherapy is efficient and flexible, and even when the tumor extends into subcutis, the treatment with plate electrode eliminated the tumor cells. This result suggests that electrochemotherapy is a suitable method to treat mast cell tumor. **Key Words:** Electrochemotherapy, Mast Cell Tumor (MCT), Numerical Simulation.

Electroporation or electropermeabilization is a phenomenon of increased permeability in the cell membrane when an intense electric field is applied (1) This effect permits efficient transport of macromolecules (even hydrophilic) inside the cells. The electroporation efficiency depends on pulse parameters (2) and cell or tissue types (cell density, shape, and orientation in relation to electric field) (3), (4), (5). The most important parameter for effective cell and tissue electroporation is adequate electric field distribution within the treated sample (6).

There are several therapies and treatments with electroporation. Some clinical applications are electrochemotherapy (reversible electroporation), tissue ablation method (irreversible electroporation), and gene therapy and DNA-based vaccination (gene electrotransfer) (6). Electrochemotherapy standard operating procedures (SOP) have been defined for the treatment of cutaneous and subcutaneous tumor nodules (8). Several studies have shown success rate of electrochemotherapy procedures in more than of 80% of cutaneous metastases of different tumor types (9).

doi:10.1111/aor.12225
Received Dec 2013; revised January 2014.
Address correspondence and reprint requests to Mrs. Daniela O. H. Suzuki, Institute of Biomedical Engineering, Federal University of Santa Catarina (UFSC),CEP 88040-900, Florianópolis-SC, Brazil.
E-mail:suzuki@ieb.ufsc.br,http://www.ieb.ufsc.br

Mast cell tumors (MCT) in dogs develop frequently in the skin, but they also grow in intestine, liver, spleen and elsewhere (10). Cutaneous MCTs compromise 11–27% of the skin tumor in dogs (10), (11). Electrochemotherapy has shown partial and complete remission in MCT (11), and has been recently suggested as an alternative to adjuvant radiotherapy for incompletely resected MCT (12). However, the outcome of the treatment depends on the position of electrodes, applied pulses, electrode geometry, and electrical properties of tissue treated (6). The numerical simulations predict or confirm these experimental findings are an important tool for the treatment planning of electroporation. Numerous studies have shown that the cell suspension conductivity is increased due to membrane electropermeabilization (2), (13). The local electric field distribution within the treated tissue also produces conductivity increase (5), (14), (15). Some authors often consider the treated tissues with constant tissue conductivities. Corociv *et al.* (15) demonstrated that nonlinear model fits better than linear model.

The aim of our study was to investigate the tumor position and dog's tissue thickness on the local electric field distribution. We compared our tumor model with an electrochemotherapy treatment in a canine mast cell tumor. This numerical study was performed using four different composite tissues.

MATERIALS AND METHODS

Case Study

The animal was a 7-year-old boxer with spontaneous nodular formation of cutaneous mast cell tumor on ear, grade II (16), with a diameter of about 5 mm. There were no clinical

symptoms. The animals were anesthetized and injected with intravenous application of bleomycin ($15{,}000\ IU/m^2$) before the application of electric pulses. Electric pulses of$1300\ V/cm$, 8 pulses, $100\ \mu s$, and $1\ Hz$ were generated with a BTX ECM 830 (Harvard Apparatus, Holliston, MA), and were delivered in single session using two parallel, stainless-steel plate electrodes of $1\times1\ cm^2$. The tumor was treated in accordance with standard operating procedures of the electrochemotherapy (8). After the treatment, the patient was clinically monitored during 1174 days (until his death), there was no cancer recurrence. The experiments were performed in agreement with the recommendations of the ethical committee.

Numerical and geometry modeling

The electric field distributions on biological tissue were computed by finite-element method (FEM) simulations using the COMSOL Multiphysics® software package. The mesh of 68,851 tetrahedral elements was generated by FEM tool.

The electric field distribution models were calculated using the steady current module. If supposing that the electric current density $\boldsymbol{J}$ in tissue is divergence-free, the solved equation is the Poisson's equation:

$$-\nabla\cdot(\sigma\nabla V)=0 \tag{1}$$

where σ is the tissue conductivity (S/m) and V is the electric potential(V).

The boundary conditions were all insulating on the external surfaces (Neuman's boundary condition). The contact between electrode and tissue was modeled as Dirichlet's boundary condition.

The geometry tries to model the electrochemotherapy *in vivo* experiment reported, as shown in Fig. 1. The electrode separation is $d=5\ mm$ and the applied voltage is $V=650\ V$, which result in an electric field magnitude of $1300\ V/cm$. The tumor model comprises four types of tissues: epidermis and stratum corneum (SC), dermis, muscle and, tumor.

Two models representing different parallel plate electrode placement situations were developed. The first model describes the electrodes touching the skin tissue just at limit tumor convexity and the second model implements the variation in tumor position and tissue thickness.

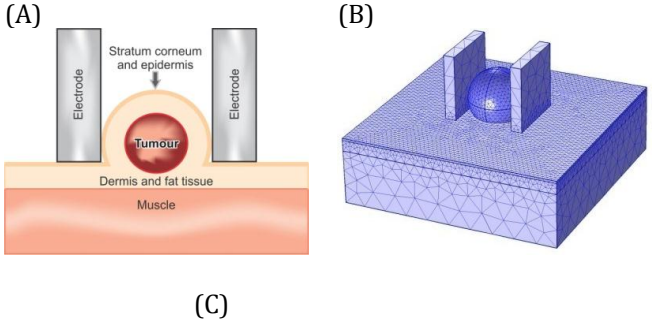

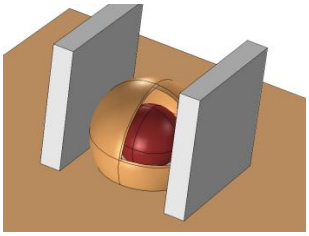

FIG.1. – Simulation of numerical model of dog tumor. (A) Tissue description; (B) mesh geometry; (C) 3D model detail, cut surface (epidermis and SC); the solid sphere is the tumor enveloped by dermis (translucent).

In the areas where electric field magnitudes are low enough, the tissue conductivity can be treated as a constant (σ_0), because the amplitude of the applied electroporation pulse is very low to produce an electric field above the reversible electroporation pulse (E_{rev}).

When the local electric field (E) in the tissue exceeds the E_{rev} value, the tissue conductivity increases owing to electroporation. Furthermore, the conductivity dependence of electric field is expressed as (17):

$$\sigma(E)=\sigma_0+\frac{\sigma_{max}-\sigma_0}{1+D.e^{-\left(\frac{E-A}{B}\right)}} \tag{2}$$

$$A=\frac{E_{irrev}+E_{rev}}{2}$$

$$B=\frac{E_{irrev}-E_{rev}}{C}$$

where σ_{max} is the maximal conductivity of permeabilized tissue, $E_{rev}$and $E_{irrev}$are reversible and irreversible threshold of electric field, respectively, and $C=8$ and $D=10$ are sigmoid function parameters (17). The values of σ_0, σ_{max}, E_{irrev} and $E_{rev}$for each tissue are presented in Table 1.

TABLE 1.
Electric parameters of electric conductivity dependency of tissue (17)

	σ_0 (S/m)	σ_{max} (S/m)	E_{rev} (kV/m)	E_{irrev} (kV/m)
Epidermis and SC	0.008	0.800	40	120
Dermis	0.250	1.000	30	120
Muscle	0.135	0.340	20	80
Tumor	0.300	0.750	40	80

Fig.2 shows the $\sigma(E)$ dependency of four tissue types (Table 1). The tissues present differences in cell size, form, and interactions. We can expect some cells to be permeabilized before the others when $E>E_{rev}$ The sigmoid function describes gradual increase in the tissue conductivity and when $E>E_{irrev}$ leads to saturation curve.

The model simulation was run on personal computer (Intel Core i5-2500, 3.3 GHz CPU, 4 GB RAM) with Windows 7 operating system.

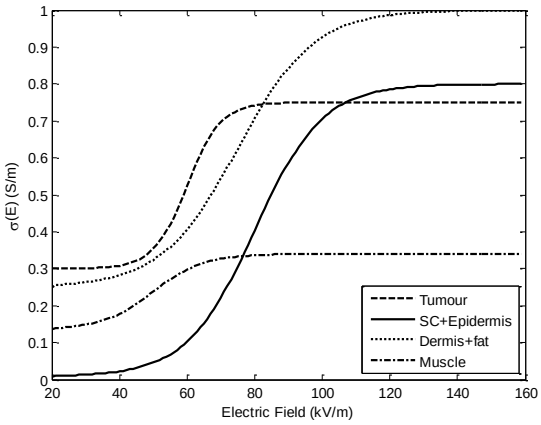

FIG. 2. – $\sigma(E)$dependency as sigmoid function of four tissues: tumor, epidermis and SC, dermis and fat, muscle.

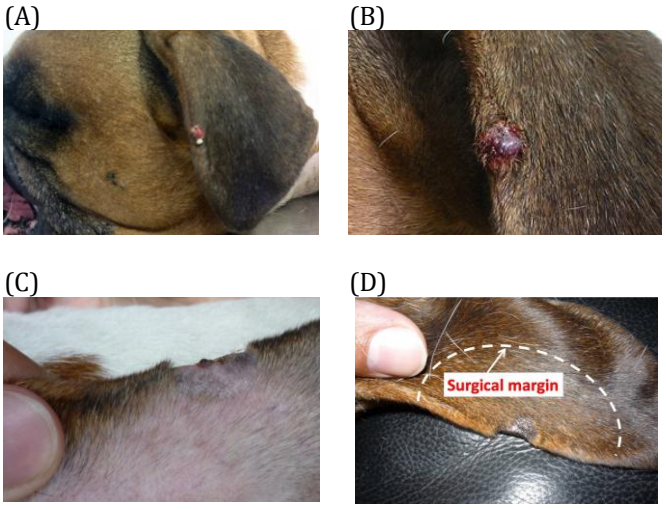

FIG. 3. – Electrochemotherapy applied to a dog tumor of 5 mm; pulses of 1300 V/cm, 8 pulses, 100 μs, and 1 Hz. (A) Before the treatment; (B) immediately after the applied electric pulse, visible necrosis areas are not observed, (C) 1 month after electrochemotherapy; (D) 2 months after treatment; only healthy tissue observed. The dotted line is the free surgical margins recommended in (10).

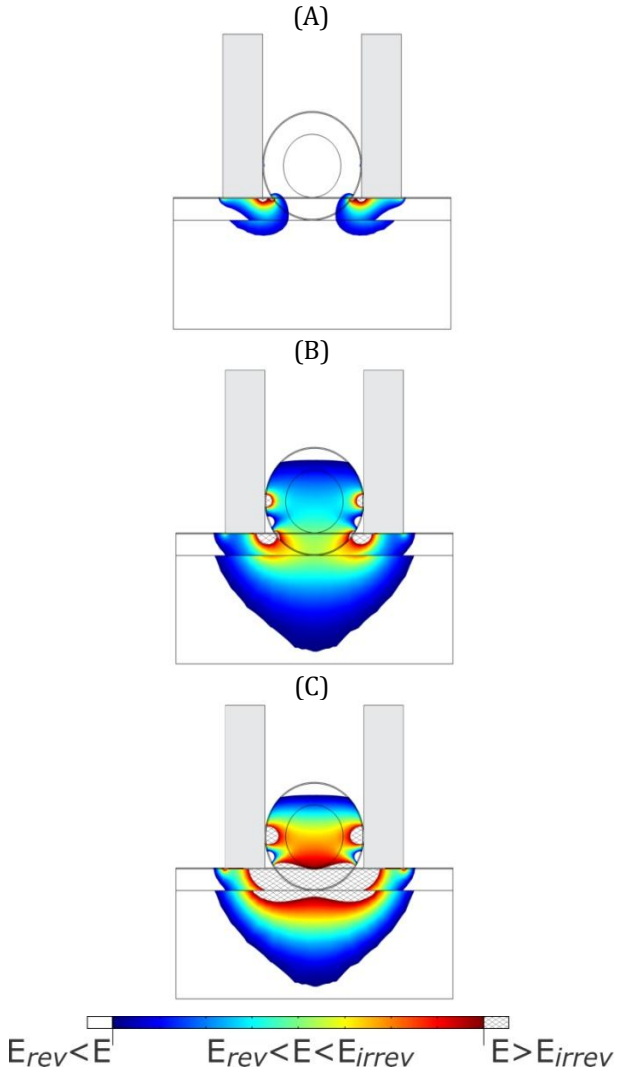

FIG. 4. – Local electric field distribution with applied voltage of 650 V (electrode distance of 5 mm). These tumors are grade I, well-differentiated superficial dermal tumors. (A) Constant conductivity in all tissues (σ_0); (B) tissue conductivity according to the model of Eq. (2); (C) there are no epidermis, SC, and dermis around the tumor; the tumor diameter is 5 mm..

RESULTS

Fig. (3A) presents the mastocytoma tumors with a diameter of about 0.5 mm. Fig. (3B), (3C), and (3D) shows the macroscopic changes on tumor observed after electrochemotherapy. No necrosis areas can be observed in Fig.(3B). Therefore, in the simulation model, if the area with E_{irrev} (necrosis area) is bigger than 5% of tumor volume, the math model will be considered as invalid. Fig. (3D) presents an effectiveness of the treatment, and no tumors can be observed. The local electric field is $E_{rev} < E < E_{irrev}$ on all tumor areas.

Fig. 4 shows the results of superficial dermal tumor model. The epidermis and SC thickness is 0.06 mm (19), dermis thickness is 1 mm (20), muscle thickness is 5 mm(21), and tumor diameter is 2.9 mm. The thickness values are applied for dogs. The three different models with: (A) tissues conductivities are constant, which is not dependent on electric field ($\sigma(E)$); (B) each tissue being modeled by Eq. (2) and data presented in Table 1; and (C) the sphere conductivity being uniform and equal to tumor, which was used in another study (22).

In Fig. 5, three different situations with different dermis thickness, tumor radius, and tumor position are presented. The epidermis and SC thickness is considered constant (0.06 mm), muscle thickness is 5 mm and the tissues conductivity is dependent on the electric field. Fig. (5A) presents dermis thickness is 0.8 mm and tumor diameter is 3.28 mm. Fig (5B) was simulated with dermis thickness is 1.5 mm and tumor diameter is 1.88 mm. The tumor radius is 0.94 mm, as showed in Fig (5C). It is difficult to determine the exact tumor position and dimension tissues. We analyzed these situations to verify the match of possibility treatment.

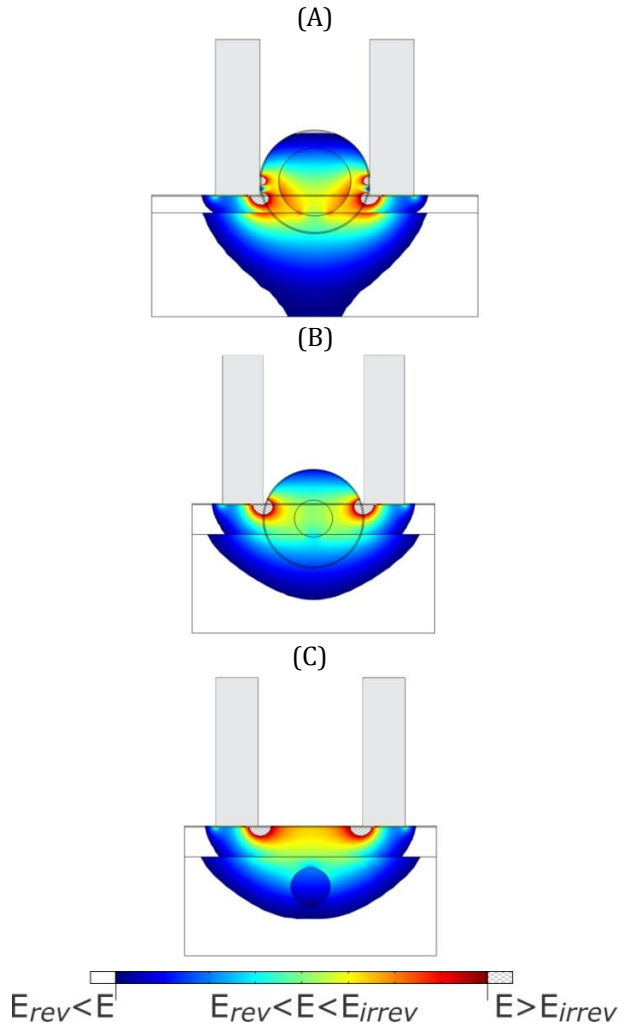

FIG. 5. – Local electric field distribution with applied voltage of $650V$ (electrode distance of 5 mm). (A) Dermis thickness is 0.8 mm, tumor diameter is 3.28 mm, epidermis is 0.06 mm, and the tumor extension to muscle is 0.2 mm (characteristic of grade II); (B) Dermis thickness is 1.5 mm, tumor diameter is 1.88 mm, and the tumor extension to muscle is 0.2 mm; (C) The subcutaneous tumor (radius is 0.94 mm) is inside the muscle (3 mm under the skin surface).

DISCUSSION

MCTs or mastocytomas are frequently seen in dogs, particularly in the skin. The treatment of choice is wide excision (3 cm free margin, Fig. 3D) eventually followed by other treatment modalities such irradiation, cortisone, and/or chemotherapy (10). The advantages of electrochemotherapy in these cases is: easy and effective treatment of single or multiple tumor nodules (7); reduction in tissue loss and good cosmetic effects obtained due to a selective cell death mechanism that primarily affects the dividing tumor cells (23); and treatment of choice for tumors refractory to conventional treatments (9).

When bleomycin is injected intravenously, the selectivity of treatment is caused by a mitotic cell death that kills the dividing tumor cells (23). The neighboring cells are affected by the electric field and bleomycin as well inside the cells; however, normal cells do not divide, explaining selectivity towards the dividing tumor cells and safety of the procedure. Another advantage is the vascular effects of the electric pulses; electrochemotherapy provokes a transient vascular lock, which prevents bleeding and even stops previous bleeding in the case of hemorrhagic nodules (7).

In dogs and cats, cutaneous MCTs are solitary or multicentric tumors that are usually confined to the dermis and/or subcutis (24). This model considers solitary, circumscribed, and superficial dermis (grade I), and extend into the deeper dermis and subcutis (grade II), as shown in Fig. 3. Although grade I is better well-differentiated tumor than grade II (24), we defined the tumor like a sphere for both the cases.

Our model utilizes the tissues electric conductivity of humans (Table 1). Gabriel *et al*. (25) observed that the electric conductivity of human and dog skin is similar. We extend this similarity to conductivity dependence of electric fields. Some works have modeled this dependency as constant (26), linear (21), and nonlinear (14), (18). The sigmoid model (17) was used in this study, because Corovic *et al*. (17) demonstrated that nonlinear models fit experimental results better than linear models. There is no definition of conductivity math model during electroporation.

For planning of the electrochemotherapy treatment, it is important to consider the conductivity variation during electroporation (14). We demonstrated the effect of planning the treatment without model electroporation in tissue, as shown in Fig. (4A). The electric field is not enough ($E < E_{rev}$) inside the tumor. The constant conductivity model does not describe the experimental result (tumor eliminated; Fig (3D)). Fig. (4B), with $\sigma(E)$, presents the electroporation effect on the electric field distribution and, consequently, on the treatment efficiency. Fig. (4C) shows the simulated results of only one tumor. This model is used in simulations of cutaneous tumor (21). The irreversible electric field is greater than 5% of tumor volumes. This result evidences the importance of dermis, epidermis and SC on our model.

The epidermis and SC are thin (typically around 0.1 mm (27)), which contributes a great deal to the electrical properties of skin. Its low conductivity makes skin one of the least conductive tissues in the human body (Table 1). The difference in the epidermis thickness depends on the dog's body, but it does not affect the electric field distribution at simulated tissues (data not shown). The epidermis and SC thickness of dogs ($0.02-0.06\ mm$ (19), (20)) are thinner than those of humans ($0.05-1\ mm$ (27)). The dermis is the second layer of skin, beneath the epidermal layer. This layer is much thicker than the epidermis; the dermis thickness of humans is 50 μm on the eyelids to 1 mm on the palms and soles, with an average thickness of 100 μm (27), whereas that of dog is 800 μm to 1.5 mm (20). As shown in Fig. (5), we verified the dermis thickness variation in dogs, and tumors invading the muscle area. The distance between the electrodes was 5 mm in all cases. Therefore, we modified the tumor radius and depth.

In the Fig. (5A), the tumor radius is 1.64 mm and it was be treated properly ($E_{rev} < E < E_{irrev}$). There small necrosis areas are limited to dermis, epidermis and SC. It might be possible that necrosis areas occur after electrochemotherapy application, but it is not visible. Fig. (5B) shows a smaller tumor than that presented in Fig. (5A) (radius of 0.94 mm) with a maximum dermis described in the literature (tumor on

the paws). Even in this case, the treatment is efficient. This result suggests that skin melanocytic tumor treatment can be applied on the entire dog body. These results thus confirm the importance of flexibility of electrochemotherapy on the cutaneous and subcutaneous tumors (8). Fig. (5C) represents a subcutaneous tumor. The irreversible electric field is localized only near the electrodes (epidermis, SC, and dermis). Some studies have shown that in these tumors, it is better to use needle electrodes (15), (22). However, if the depth of the tumor is less than $3\,mm$, the plate electrodes can be used (6). We estimated that the results presented in Fig. (5A) are close to reality, because the ear dermis is more consistent with $0.8\,mm$.

CONCLUSION

In this study, we compared the electrochemotherapy treatment of dog mast cell tumor using plate electrodes and possible variations in thickness tissues and tumor positions. We demonstrated that the structural variations of dog tissues, dermis between 0.8 and $1.5\,mm$, and even subcutaneous tumors ($depth < 3\,mm$) permit efficient treatment (*i.e.*, the local electric field is enough to permit bleomycin inside the tumoral cells). If mast cell tumor is extended into subcutis, electrochemotherapy will eliminate these tumor cells at depth less than $3\,mm$. These results confirm the flexibility and efficiency of electrochemotherapy and the protocols proposed by Marty *et al.*(8).

Conflict of Interest: We declare that we have no conflict of interest.

REFERENCES

1. J. Teissié, M. Golzio, and M. P. Rols, "Mechanisms of cell membrane electropermeabilization: A minireview of our present (lack of?) knowledge," *Biochim. Biophys. Acta*, vol. 1724, pp. 270–280, 2005.
2. D. O. H. Suzuki, A. Ramos, M. C. M. Ribeiro, L. H. Cazarolli, F. R. M. B. Silva, L. D. Leite, and J. L. B. Marques, "Theoretical and experimental analysis of electroporated membrane conductance in cell suspension.," *IEEE transactions on bio-medical engineering*, vol. 58, no. 12, pp. 3310–8, Dec. 2011.
3. A. Ramos, D. O. H. Suzuki, and J. L. B. Marques, "Numerical simulation of electroporation in spherical cells.," *Artificial organs*, vol. 28, no. 4, pp. 357–61, Apr. 2004.
4. D. O. H. Suzuki, A. Ramos, and J. L. B. Marques, "Modeling Environment for Numerical Simulation of Applied Electric Fields on Biological Cells," *Electromagnetic Biology and Medicine*, vol. 23, no. 3, pp. 239–250, 2007.
5. S. Corović, A. Zupanic, S. Kranjc, B. Al Sakere, A. Leroy-Willig, L. M. Mir, and D. Miklavcic, "The influence of skeletal muscle anisotropy on electroporation: in vivo study and numerical modeling.," *Medical & biological engineering & computing*, vol. 48, no. 7, pp. 637–48, Jul. 2010.
6. S. Corovic, J. Bester, and D. Miklavcic, "An e-learning application on electrochemotherapy.," *Biomedical engineering online*, vol. 8, p. 26, Jan. 2009.
7. S. T. Kee, J. L. Gehl, J. Lee, W. Edward, *Clinical Aspects of Electroporation*. New York, NY: Springer New York, 2011.
8. M. Marty, G. Sersa, J. R. Garbay, J. Gehl, C. G. Collins, M. Snoj, V. Billard, P. F. Geertsen, J. O. Larkin, D. Miklavcic, I. Pavlovic, S. M. Paulin-Kosir, M. Cemazar, N. Morsli, D. M. Soden, Z. Rudolf, C. Robert, G. C. O'Sullivan, and L. M. Mir, "Electrochemotherapy – An easy, highly effective and safe treatment of cutaneous and subcutaneous metastases: Results of ESOPE (European Standard Operating Procedures of Electrochemotherapy) study," *European Journal of Cancer Supplements*, vol. 4, no. 11, pp. 3–13, Nov. 2006.
9. G. Sersa, J. Gehl, J.-R. Garbay, D. M. Soden, G. C. O'Sullivan, L. W. Matthiessen, M. Snoj, and L. M. Mir, "Electrochemotherapy of Small Tumors; The Experience from the ESOPE (European Standard Operating Procedures for Electrochemotherapy) Group," in in *Clinical Aspects of Electroporation*, S. T. Kee, E. W. Lee, and J. Gehl, Eds. New York: Springer New York, 2011, pp. 93–102.
10. W. Misdorp, "Mast cells and canine mast cell tumours. A review.," *The Veterinary quarterly*, vol. 26, no. 4, pp. 156–69, Dec. 2004.
11. V. Kodre, M. Cemazar, J. Pecar, G. Sersa, A. Cor, and N. Tozon, "Electrochemotherapy compared to surgery for treatment of canine mast cell tumours.," *In vivo (Athens, Greece)*, vol. 23, no. 1, pp. 55–62, 2009.
12. E. P. Spugnini, B. Vincenzi, F. Baldi, G. Citro, and A. Baldi, "Adjuvant electrochemotherapy for the treatment of incompletely resected canine mast cell tumors.," *Anticancer research*, vol. 26, no. 6B, pp. 4585–9, 2006.
13. A. Ramos, A. L. S. Schneider, D. O. H. Suzuki, and J. L. B. Marques, "Sinusoidal signal analysis of electroporation in biological cells.," *IEEE transactions on bio-medical engineering*, vol. 59, no. 10, pp. 2965–73, Oct. 2012.
14. A. Ramos, "Effect of the Electroporation in the Field Calculation in Biological Tissues," *Artificial organs*, vol. 29, no. 6, pp. 510–513, Jun. 2005.
15. S. Corovic, I. Lackovic, P. Sustaric, T. Sustar, T. Rodic, and D. Miklavcic, "Modeling of electric field distribution in tissues during electroporation," *Biomedical engineering online*, vol. 12, no. 1, p. 16, Jan. 2013.
16. A. K. Patnaik, W. J. Ehler, and E. G. Macewen, "Canine cutaneous mast cell tumor: morphologic grading and survival time in 83 dogs," *Veterinary Pathology*, vol. 21, pp. 469–474, 1984.
17. D. Miklavcic, D. Sel, D. Cukjati, D. Batiuskaite, T. Slivnik, and L. Mir, "Sequential finite element model of tissue electropermeabilisation," *IEEE Transactions on Biomedical Engineering.*, vol. 52, no. 5, pp. 816–827, Jan. 2005.
18. S. Corovic, I. Lackovic, P. Sustaric, T. Sustar, T. Rodic, and D. Miklavcic, "Modeling of electric field distribution in tissues during electroporation.," *Biomedical engineering online*, vol. 12, no. 1, p. 16, Jan. 2013.
19. N. A. Monteiro-Riviere, D. G. Brsitol, T. O. Manning, R. A. Rogers, and J. E. Riviere, "Interspecies and interregional analysis of the comparative histologic thickness and laser Doppler blood flow measurements at five cutaneous sites in nine species," *Journal of Investigative Dermatology*, vol. 95, no. 5, pp. 583–586, 1990.
20. J. Bhandal, I. M. Langohr, D. a Degner, Y. Xie, B. J. Stanley, and R. Walshaw, "Histomorphometric analysis and regional variations of full thickness skin grafts in dogs.," *Veterinary surgery : VS*, vol. 41, no. 4, pp. 448–54, May 2012.
21. A. Ivorra, B. Al-Sakere, B. Rubinsky, and L. M. Mir, "Use of conductive gels for electric field homogenization increases the antitumor efficacy of electroporation therapies.," *Physics in medicine and biology*, vol. 53, no. 22, pp. 6605–18, Nov. 2008.
22. S. Corovic, B. Al Sakere, V. Haddad, D. Miklavcic, and L. M. Mir, "Importance of contact surface between electrodes and treated tissue in electrochemotherapy.," *Technology in cancer research & treatment*, vol. 7, no. 5, pp. 393–400, Oct. 2008.
23. L. M. Mir, "Bases and rationale of the electrochemotherapy," *European Journal of Cancer Supplements*, vol. 4, no. 11, pp. 38–44, Nov. 2006.
24. H. M. Meuten D, Goldschmidt MH, "Tumors of the skin and soft tissues," in in *Tumors in Domestic Animals*, 4th ed., D. J. Meuten, Ed. Ames, Iowa, EUA: Iowa State Press, 2002, pp. 45–117.
25. C. Gabriel, S. Gabriel, and E. Corthout, "The dielectric properties of biological tissues: I. Literature survey.," *Physics in medicine and biology*, vol. 41, no. 11, pp. 2231–49, Nov. 1996.
26. D. Semrov and D. Miklavcic, "Numerical Modeling for In Vivo Electroporation," in in *Electrochmeotherapy, Electrogenetherapy, and Transdermal Drug Delivery*, M. J. Jaroszeski, R. Heller, and R. Gilbert, Eds. Totowa, New Jersey: Humana Press, 1999, pp. 63–82.
27. J. Kanitakis, "Anatomy , histology and immunohistochemistry of normal human skin," *European Journal of Dermatology*, vol. 12, no. 4, pp. 390–401, 2002.